Nonuniformity of Reaction Through Flooded Porous Electrodes

LEONARD G. AUSTIN and EUGENE G. GAGNON

Department of Materials Science
Pennsylvania State University, University Park, Pennsylvania 16802

The theoretical description of the behavior of porous electrode systems has received much study in the past few years (*1*). In essence, all of the treatments consist of combining kinetic and transport equations for postulated models of behavior and geometry. The concepts and techniques used are similar to kinetic and transfer studies in porous catalysts, but with the added effect of voltage in the electrochemical system. This paper is a more complete study than previously available of the particular case of flooded, plane, porous electrodes, with experimental proof of some of the derived equations.

ASSUMPTIONS AND DESCRIPTIVE EQUATIONS

The basic equations for a plane, porous electrode have been derived several times (*2*), and only a brief review will be given here. It is assumed that the porous system is so highly interlinked that the concentration of species dissolved in the electrolyte flooding the pores of the electrode is constant over plane x in the electrode (see Figure 1). Similarly, the electrode potential is constant over plane x. It is further assumed that the transport gradients are one-dimensional (along x), which is true when the thickness (L) of the electrode is much greater than the pore diameters. It is assumed that the electronic conductivity of the electrode material is large compared to the ionic conductivity of the electrolyte within the pores, so that the potential of the electrode material is constant along x. The electrolyte is assumed to be concentrated, so that the thickness of the double layer is a few angstroms only and, hence, the double layer covers the internal surface area of the electrode and no diffuse double-layer effects are present. All of these assumptions are reasonable for many cases of practical interest.

Electrode potential V is defined as the potential of the electrode solid ψ_M minus the potential of the electrolyte ψ_E, that is, $V = \psi_M - \psi_E$. Current is supported by transport of ions in the electrolyte and, hence, a potential gradient $d\psi_E/dx$ exists in the electrolyte. Clearly, for constant ψ_M

$$dV/dx = d(\psi_M - \psi_E)/dx = -d\psi_E/dx$$

It is convenient to work in terms of polarization η, which is variation of electrode potential from the reversible potential of the electrode V_r, that is, $\eta = \pm (V_r - V)$. With the use of the European sign convention that $V = \psi_M - \psi_E$, net anodic current is produced when V is more positive than V_r, that is, $\eta_{\text{anodic}} = V - V_r$, and cathodic current is produced by more negative V, $\eta_{\text{cathodic}} = V_r - V$. Thus η is chosen positive for the current direction of interest and identical equations are obtained for an anode or a cathode. An illustration of the potential gradients of an anode and cathode is given in Figure 2.

Considering a cathodic reaction, the electrode current (flow of positive charge out of electrode solid) produced by electrochemical reaction between 0 and x is supported by the flow of the ions across plane x, and since electrolytes obey Ohm's Law,

$$i(x) = (1/\rho)d\psi_E(x)/dx = -(1/\rho)dV(x)/dx = (1/\rho)d\eta_c(x)/dx$$

Similarly, for an anodic reaction, the positive charge flowing into the electrode solid between 0 and x from the external circuit is

$$i(x) = -(1/\rho)d\psi_E(x)/dx = (1/\rho)d\eta_a(x)/dx$$

The equations may be expressed as

$$i(x) = (1/\rho)d\eta(x)/dx \qquad (1)$$

where i is anodic or cathodic, depending on whether η is anodic or cathodic. It is convenient to express i as current density per unit area of plane x, that is, per unit geometric area of electrode. Then ρ is effective specific resistance of the electrolyte contained within the porosity of the electrode, per unit area of electrode and $\rho = \lambda\rho_{\text{free}}$, where

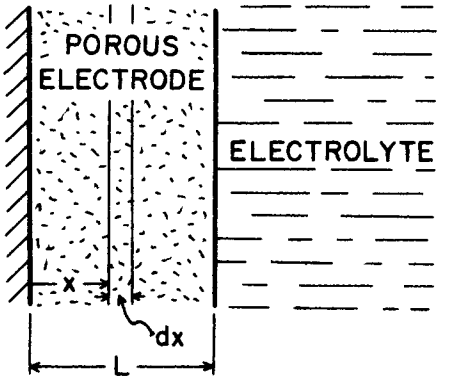

Fig. 1. Illustration of a porous electrode with one face exposed to the electrolyte.

Correspondence concerning this article should be addressed to Dr. Eugene G. Gagnon, G. M. Laboratories, Warren, Michigan 48090.

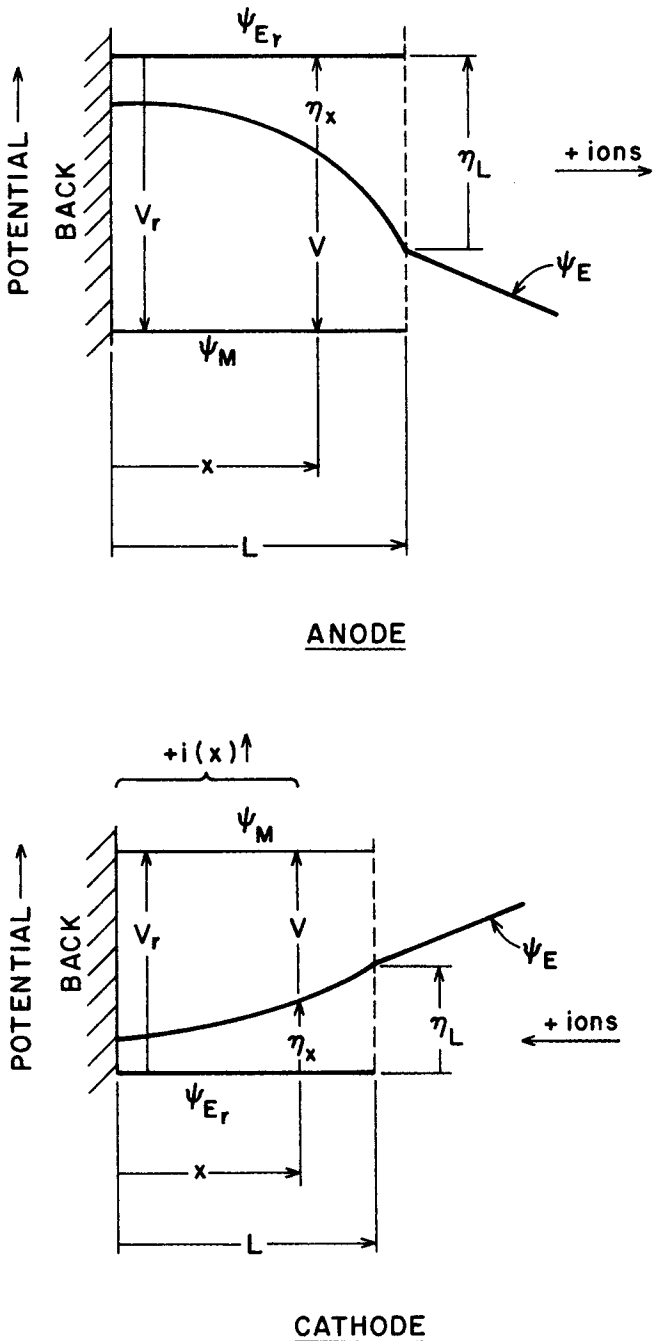

Fig. 2. Illustration of the potential gradients in a porous anode and cathode.

ρ_{free} is the true specific resistance of the electrolyte and λ is a labyrinth factor dependent on porosity and tortuosity.

Not only must the electrochemical reaction be supported by flow of ions, but appropriate mass transfer of the reactants and products must occur. As a reasonable approximation (3) it can be assumed that the mass transfer of the reactant in the electrolyte across plane x is described by Fick's law:

$$\text{flux rate in direction } x = -DdR(x)/dx \qquad (2)$$

where $R(x)$ is the concentration of reactant at x. Again, D is an effective diffusion coefficient $D = D_{free}/\lambda$. For a charged species, D_{free} is near in value to the polarographic diffusion coefficient, but the exact value is dependent on the other ions present (3).

It is now possible to relate the variation of η with x to the variation of R with x. Since the current produced by electrochemical reaction between 0 and x has to be supported by the flux of reactant through plane x toward the interior, Equation (2) gives $i(x) = nFDdR(x)/dx$, where nF is the coulombs per gram-mole of reactant. Combining with Equation (1)

$$(1/\rho)d\eta(x) = nFDdR(x) \qquad (3)$$

In general ρ will vary with x since it may vary with R. Two limiting cases exist. For concentrated electrolytes, strongly supported electrolytes, or where R is not a charged species, the resistance of the electrolyte may remain almost constant as R varies. Then, integrating with the boundary conditions of $R = R(L)$, $\eta = \eta(L)$, at $x = L$, one gets

$$\eta(L) - \eta(x) = \rho nFD\,[R(L) - R(x)] \qquad (4)$$

The other limit is an electrolyte where $\rho \propto 1/R$, and

$$R(x)/R(L) = \exp\left\{\frac{-1}{nFDR(L)\rho(L)}\,[\eta(L) - \eta(x)]\right\} \qquad (5)$$

Note that these relations are independent of the kinetics of the electrochemical reaction.

It now remains to combine the above effects of potential gradient due to Ohm's law, and variation of R due to mass transfer, with an electrochemical kinetic expression. The kinetic expression chosen is the usual simple one of

$$i = i_o\left\{(R/R_b)\exp\left(\frac{\alpha\eta}{b}\right) - (P/P_b)\exp\left(\frac{-(1-\alpha)\eta}{b}\right)\right\} \qquad (6)$$

The element of electrode volume dx thick with unit cross-sectional area contains a reactive area of Sdx, where S is the specific reactive area (sq.cm./cu.cm.) of the electrode. Thus the current produced by electrochemical reaction in this element of volume $di(x)$ is given by

$$di(x) = i_o S\left\{\left(\frac{R(x)}{R_b}\right)\exp\left(\frac{\alpha\eta}{b}\right) - \left(\frac{P(x)}{P_b}\right)\exp\left(\frac{-(1-\alpha)\eta}{b}\right)\right\}dx$$

Differentiating Equation (1) with respect to x and combining with the above, one obtains

$$d\eta^2(x)/dx^2 = i_o S\rho\left\{\left(\frac{R(x)}{R_b}\right)\exp\left(\frac{\alpha\eta}{b}\right) - \left(\frac{P(x)}{P_b}\right)\exp\left(\frac{-(1-\alpha)\eta}{b}\right)\right\} \qquad (7)$$

This is the basic equation to be solved for various conditions. In general it should also be combined with a heat transfer equation, but it is assumed here that the system is isothermal. The useful potential of the electrode corresponds to $\eta(L)$, so it is necessary to express solutions in terms of $\eta(L)$.

SOLUTIONS FOR NEAR REVERSIBLE REACTION

Near reversible reaction is defined as reaction at low values of η, that is, electrode potentials close to the reversible potential. Equation (4) can be rearranged to

$$\frac{R(x)}{R_b} = \frac{R(L)}{R_b} - \frac{\eta(L) - \eta(x)}{\rho n \mathcal{F} D R_b}$$

This equation is also obtained from Equation (5) as the limit when η is small. Substituting for $R(x)/R_b$ in Equation (7), for low values of η (using $\exp x = 1 + x + x^2/2! + \ldots$, neglecting the x^2 and higher terms), and assuming negligible external mass transfer effects [that is, $R(L)/R_b = P(L)/P_b = 1$], one gets

$$d^2\eta(x)/dx^2 = i_o S\rho \left[\left(\frac{\alpha + \phi}{\phi} \right) \eta(x) - \left(\frac{\alpha}{\phi b} \right) \eta(L) \right]$$

where

$$\phi = \alpha \rho n \mathcal{F} D R(L)/b \qquad (8)$$

In addition to the algebraic convenience of combining terms into ϕ, the value of the dimensionless group ϕ is an important criterion for deciding whether ohmic or mass transfer effects predominate in producing nonuniform reaction in the electrode (*4*). Solution with the boundary conditions $d\eta(x)/dx = 0$ at $x = 0$, $\eta = \eta(L)$ at $x = L$ gives

$$\frac{A\eta(x) - B}{A\eta(L) - B} = \frac{\exp(x\sqrt{A}) + \exp(-x\sqrt{A})}{\exp(L\sqrt{A}) + \exp(-L\sqrt{A})}$$

where

$$A = i_o S\rho(\alpha + \phi)/\phi b$$

$$B = i_o S\rho\alpha\eta(L)/\phi b$$

The relation between ionic current passing through the plane at x (current produced by reaction from 0 to x) and $\eta(L)$ is readily obtained from $i(x) = (1/\rho)d\eta(x)/dx$:

$$i(x) = \left(\frac{i_o S\eta(L)}{b\sqrt{A}} \right) \left(\frac{\exp(x\sqrt{A}) - \exp(-x\sqrt{A})}{\exp(L\sqrt{A}) + \exp(-L\sqrt{A})} \right) \qquad (9)$$

The working equations and limiting cases derived from Equation (9) are shown in Table 1, where the total current $i(L)$ is denoted by i and the total polarization $\eta(L)$ is denoted by η_L.

SOLUTIONS FOR IRREVERSIBLE REACTION

When the true exchange current and the specific area is relatively low, most of the reaction will occur under irreversible conditions (η large) and the limiting case is when the second, reverse, term in Equation (7) can be neglected at all penetrations in the electrode. Equation (7) then goes to

$$d\eta^2(x)/dx^2 = i_o S\rho[R(x)/R_b] \exp[\alpha\eta(x)/b]$$

The variable term $R(x)/R_b$ is replaced in terms of $\eta(x)$, $\eta(L)$ using either of the cases represented by Equations (4) and (5). The solution of the above equation with Equation (5) has been given (*5*) and leads to

$$d\eta(x)/dx = (2A/\rho)\,[\exp(p\eta) - \exp(p\eta_0)]^{1/2} \qquad (10)$$

where

$\eta = \eta(x)$; $\eta_0 = \eta(0)$; $\eta_L = \eta(L)$, and

$$A = i_o S\rho(R_L/R_b) \exp\left[\left(\frac{\alpha}{b} - p \right) \eta_L \right]$$

$$p = \frac{\alpha}{b}\left(1 + \frac{1}{\phi} \right)$$

From $i(x) = (1/\rho)d\eta(x)/dx$

$$i(x) = \sqrt{(2A/p\rho^2)}\,[\exp(p\eta) - \exp(p\eta_0)]^{1/2} \qquad (11)$$

Integration of Equation (10) gives

$$\exp[p(\eta - \eta_0)] = \sec^2[x\sqrt{(A\rho/2)\exp(p\eta_0)}] \qquad (12)$$

These equations immediately give

$$i = (2A/p\rho^2)[\exp(p\eta_L) - \exp(p\eta_0)]^{1/2} \qquad (13)$$

$$\exp[p(\eta_L - \eta_0)] = \sec^2[L\sqrt{(Ap/2)\exp(p\eta_0)}] \qquad (14)$$

For specified parameters, i_oS, L, α, b, D, ρ, and for $R_L/R_b = 1$ (or known as a function of i), ϕ and p can be calculated. Equation (14) is a relation between η_L and η_0 which

TABLE 1. LIMITING CASES FOR NONUNIFORM REACTION EQUATIONS

Conditions	Current-polarization relation	Limiting conditions		Apparent exchange current density $I_A =$	Fraction of reaction from 0 to x $i(x)/i =$
Near-reversible	$i = I_A\eta_L/b$,	Ohmic and mass transfer affected		$(i_oSL)\dfrac{\tanh[L\sqrt{i_oS\rho(\alpha+\phi)/\phi b}]}{[L\sqrt{i_oS\rho(\alpha+\phi)/\phi b}]}$	$\dfrac{\sinh(x\sqrt{i_oS\rho(\alpha+\phi)/\phi b})}{\sinh(L\sqrt{i_oS\rho(\alpha+\phi)/\phi b})}$
		$L\sqrt{i_oS\rho(\alpha+\phi)/\phi b}$	<0.3	i_oSL	x/L
			>2	$\sqrt{i_oS\rho(\alpha+\phi)/\phi b}$	$\exp[-(L-x)\sqrt{i_oS\rho(\alpha+\phi)/\phi b}]$
	I_{A1}	ohmic affected, $\phi > 5$,		$i_oSL\dfrac{\tanh[L\sqrt{i_oS\rho/b}]}{L\sqrt{i_oS\rho/b}}$	$\dfrac{\sinh(x\sqrt{i_oS\rho/b}}{\sinh(L\sqrt{i_oS\rho/b}}$
		$L\sqrt{i_oS\rho/b}$	<0.3	$i_oSL.$	$x/L.$
			>2	$\sqrt{i_oSb/\rho}$	$\exp[-(L-x)\sqrt{i_oS\rho/b}]$
		Mass transfer affected, $\phi < 0.05$		$i_oSL\dfrac{\tanh[L\sqrt{i_oS/n\mathcal{F}DR_b}]}{L\sqrt{i_oS/n\mathcal{F}DR_b}}$	$\dfrac{\sinh(x\sqrt{i_oSn\,DR_b})}{\sinh(L\sqrt{I_oSn\,DR_b})}$
		$L\sqrt{i_oS/n\,DR_b}$	<0.3	i_oSL	x/L
			<2	$\sqrt{i_oSn\mathcal{F}DR_b}$	$\exp[-(L-x)\sqrt{I_oSn\,DR_b}]$
Irreversible				i_oSL	x/L
Low current	$i = I_A\exp(\alpha\eta_L/b)$, I_{A2}			$\sqrt{\dfrac{2i_oSb(R_L/R_b)\phi}{\rho\alpha(1+\phi)}}$	
High current $\exp(p\eta_0)$ negligible compared to $\exp(p\eta_L)$	$i = I_A\exp(\alpha\eta_L/2b)$ I_{A3}	Ohmic and mass transfer		$I_A = I_O = \sqrt{2i_oSb/\rho\alpha}$	Figure 3, $i(x)/i$ = function $(x/L, i/i_c)$
		Ohmic affected, $\phi > 5$		$I_A = I_M = \sqrt{2i_oSn\mathcal{F}DR_b}$	
		Mass transfer affected, $\phi < 0.05$			

enables η_L to be calculated for any value of η_0; then Equation (13) gives i for this value of η_L. Unfortunately the equations are awkward and require trial-and-error solution.

Simpler limiting cases are obtained as approximations to the full solutions, as shown in Table 1. One limit is obtained for low currents for which $L\sqrt{(Ap/2)\exp(p\eta_0)}$ is small. This can be seen by combining Equations (13) and (14) to give

$$i = \sqrt{(2A/p\rho^2)\exp(p\eta_0)}\ \tan\left[L\sqrt{(Ap/2)\exp(p\eta_0)}\right];$$

for low values of X, $\tan X = X$ and for low i (but still irreversible), $\eta_L \sim \eta_0$ and

$$i = i_o SL(R_L/R_b)\exp(\alpha\eta_L/b) \qquad (15)$$

This is the expected normal form of the Tafel equation; when no external mass transfer is present, $R_L/R_b = 1$ and the slope is α/b and exchange current $i_o SL$. This form is only obtained when $i_o SL$ is smaller than I_{A3} (see later discussion). The other limit is the irreversible, high current case (see Table 1). For $R_L = R_b$, I_O is the pure ohmic-affected apparent exchange current (2), accurate to within 10% when $\phi \geq 5$. Note that the current-polarization equation is a Tafel equation with double the normal slope. Similarly, I_M is produced by mass transfer effects. Note that although $\exp(p\eta_0)$ is assumed negligible compared to $\exp(p\eta_L)$, $\eta_L - \eta_0$ can be small when p is large, which is the case for small ϕ. Thus in this limit there is little change in η through the electrode.

The important and useful concept of the crossover current can now be introduced. This is defined as the current at which the normal Tafel line [Equation (15)] crosses the Tafel line with doubled slope:

$$i_c = I_{A2}\exp(\alpha\eta_{Lc}/b) = I_{A3}\exp(\alpha\eta_{Lc}/2b)$$

Then

$$i_c = I^2_{A3}/I_{A2}$$

$$i_c = \left(\frac{2b}{\alpha\rho L}\right)\left(\frac{\phi}{1+\phi}\right) = \frac{2}{\rho Lp} \qquad (16)$$

Note that the kinetic parameter i_oS does not occur in this expression, so i_c can be estimated from physical parameters. This means that a design decision can be made to select an operating value of i less than i_c, and this will ensure that the electrode is only slightly affected by nonuniformity of reaction in the electrode. This decision can be made without knowledge of i_oS, providing the electrode has an irreversible, current-polarization law (see below). For ϕ large, $i_c = 2b/\alpha L\rho$; for ϕ small, $i_c = 2nFDR_L/L$.

Finally, the fraction of reaction occurring between 0 and x can be readily estimated, as follows. Equations (11) and (12) can be combined to give

$$i(x) = \sqrt{(2A/p\rho^2)\exp(p\eta_0)}\ \tan\left[x\sqrt{(Ap/2)\exp(p\eta_0)}\right]$$

Using $i_c = 2/\rho Lp$

$$i/i_c = X\tan X$$

where

$$X = L\sqrt{(Ap/2)\exp(p\eta_0)}$$

Also

$$i(x)/i = \tan\left(\frac{x}{L}X\right) \Big/ \tan X \qquad (17)$$

Thus for some value of X, i/i_c is calculated; for the same value of X, $i(x)/i$ is calculated as a function of x/L. The result is given in Figure 3, which enables $i(x)/i$ to be obtained for any i/i_c, by interpolation. As expected, for $i/i_c < 0.01$, $i(x)/i$ is a straight line of slope 1, showing uniform reaction through the electrode. As i/i_c becomes large, the reaction is concentrated in the region near the outer face. Again, no knowledge of i_oS is required.

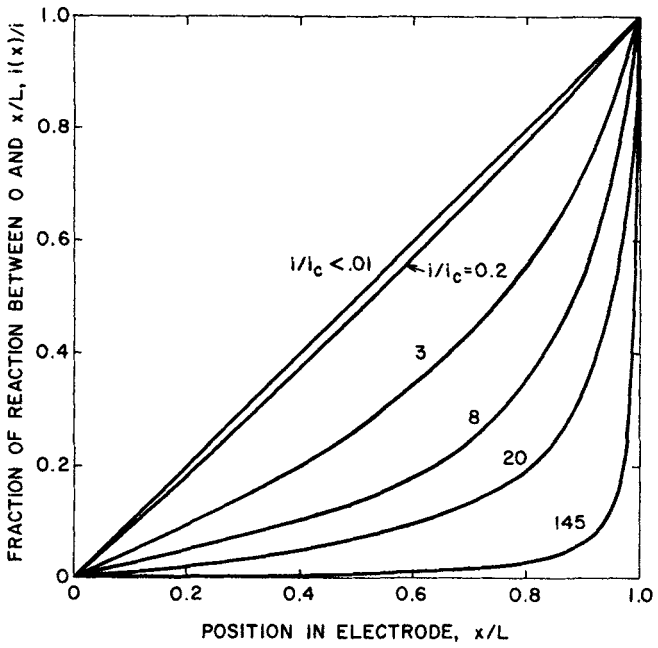

Fig. 3. Computed values of fraction of total current supported by reaction between 0 and x/L, i(x)/i, versus x/L, as a function of i/i_c.

However, at low values of i the system may tend to the reversible form which does contain the kinetic parameter i_oS, and whichever result from Figure 3 or the reversible form (see Table 1) gives the most departure of $i(x)/i$ from x/L is the result which will apply. In fact, in order for a region of uniform reaction to exist in the electrode at all, it is obviously necessary that the near-reversible stipulation for uniform reaction be satisfied in addition to $i < i_c$. Using this stipulation it is possible to obtain a ratio of I_{A2}/I_{A3} below which the near-reversible stipulation is automatically met, as follows. The reaction is virtually uniform through the electrode for the reversible form when

$$L\sqrt{i_oS\rho(\alpha+\phi)/\phi b} < 0.3.$$

But

$$I_{A3}/i_c = L\sqrt{i_oS\alpha\rho(1+\phi)/2b\phi},$$

thus

$$(I_{A3}/i_c)\sqrt{2(\alpha+\phi)/\alpha(1+\phi)} < 0.3.$$

Then, since $i_c = I^2_{A3}/i_oSL$, uniform reaction can be obtained when

$$I_{A2}/I_{A3} < 0.3\sqrt{\alpha(1+\phi)/2(\alpha+\phi)} \qquad (18)$$

For $\alpha \simeq \frac{1}{2}$, ϕ large, I_{A2}/I_{A3} should be less than about 0.15 for uniform reaction; for ϕ small, I_{A2}/I_{A3} should be less than about 0.1. Hence if $I_{A2}/I_{A3} < 0.1$, then Figure 3 can be used even at low values of i/i_c. If not, the near-reversible forms should be used at low currents because the crossover current analysis only applies when the crossover occurs at positive values of η_L, that is, $I_{A2} << I_{A3}$. If this is not true, the near-reversible form of current-polarization equation runs directly into the doubled-Tafel slope region, with no region of single-Tafel slope.

WORKING EQUATIONS

The complete current-polarization equations given above were reduced to a simpler form for the special case of ϕ large, that is, where mass transfer effects are small

compared to ohmic gradient effects in the pores. This case corresponds to the conditions of the experiments discussed below. When ϕ is large compared to unity

$$p = \frac{\alpha}{b}\left(1 + \frac{1}{\phi}\right) \simeq \alpha/b$$

It can then be readily shown that Equations (11) and (12) become

$$i(x) = \sqrt{2i_oSb/\rho\alpha}\,[\exp(\alpha\eta/b) - \exp(\alpha\eta_0/b)]^{1/2}$$

$$\exp[(\alpha/b)(\eta - \eta_0)] = \sec^2[x\sqrt{(i_oS\rho\alpha/2b)\exp(\alpha\eta_0/b)}]$$

As before

$$\left.\begin{aligned} i/i_c &= X\tan X \\ \text{where}\quad X &= L\sqrt{(i_oS\alpha\rho/2b)\exp(\alpha\eta_0/b)} \end{aligned}\right\} \qquad (19)$$

and

$$(\alpha/b)\eta_L - (\alpha/b)\eta_0 = 2\ln(\sec X) \qquad (20)$$

From Equation (19)

$$\alpha\eta_0/b = 2\ln X - 2\ln[L\sqrt{i_oS\alpha\rho/2b}] \qquad (21)$$

Equations (19) to (21) enable the polarization versus current curve for this particular case to be plotted in a general dimensionless form, as follows. Equation (21) is

$$\bar{\eta}_0 = \alpha\eta_0/b - 2\ln[1/L\sqrt{i_oS\alpha\rho/2b}] = 2\ln X \quad (21a)$$

where $\bar{\eta}$ is dimensionless polarization measured from a starting point of $2\ln[1/L\sqrt{i_oS\alpha\rho/2b}]$. For irreversible reactions, $L\sqrt{i_oS\alpha\rho/2b}$ will be small. Equation (19) shows that for positive values of current, X lies between 0 and $\pi/2$. By choosing a series of X values in this range, $\bar{\eta}_0$ is calculated. From Equation (20)

$$\bar{\eta}_L - \bar{\eta}_0 = 2\ln(\sec X) \qquad (20a)$$

Since for any value of X, $\bar{\eta}_0$ is determined, $\bar{\eta}_L$ is determined; from Equation (19), i/i_c is determined. Figure 4 shows this generalized plot. As expected from previous discussions, the result consists of two Tafel lines—one of normal slope, the other of doubled slope—joined by a transition region. In using the simple forms of intersecting Tafel lines, the shape and extent of the transition zone between them can be estimated from Figure 4.

It will be remembered that for this case, the apparent exchange current for the normal Tafel slope region at low currents (but still irreversible) is $I_{A2} = i_oSL$, and for the other region, $I_{A3} = I_O = \sqrt{2i_oSb/\rho\alpha}$. Also, $i_c = 2b/\alpha L\rho$, and $i(x)/i$ is related to i/i_c by Figure 3.

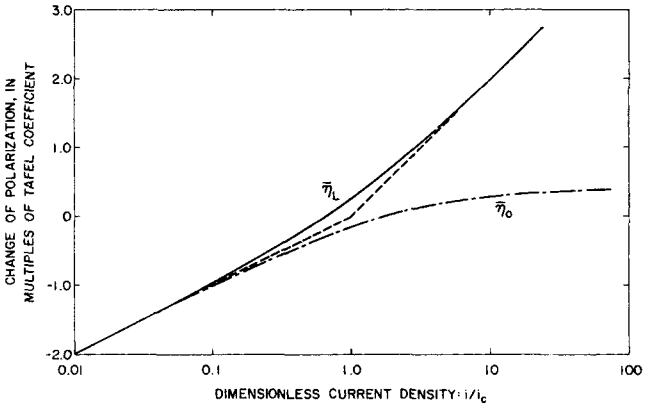

Fig. 4. Plot of dimensionless polarization $\bar{\eta}$ ($\bar{\eta}_0$ at $x = 0$ and $\bar{\eta}_L$ at $x = L$) versus i/i_c.

TEST PROCEDURES

The experimental arrangement used in this study has been described in detail in an earlier paper (6). The electrode used was the Harry Diamond Laboratory electrode, which consists of fine particles of silver ($\sim 1\mu$) sintered onto expanded-metal (Exmet) screen and electroformed to approximately 50:50 wt% of Ag and Ag_2O, with an electrode thickness of 10 mil (0.25 mm.) and porosity of about 70%. The electrodes were mounted in a Teflon holder with one face of about 1/3 sq. cm. exposed to the electrolyte. A current collector was press-fitted against the sealed back of the electrode. They were tested in 31 wt% (eutectic) KOH using conventional half-cell techniques. A Hg-HgO/KOH reference electrode with a Luggin capillary was used and the tip of the capillary was positioned very close to the surface of the test electrode. The test cell was contained in a Tenney (model TJR) constant-temperature cabinet and measurements were performed from room temperature to −62°C. (−80°F.). The low temperatures enabled a wide range of exchange currents to be investigated.

The electrodes were cathodically discharged using a galvanostatic technique that made use of a rapid switching, Hg-wetted relay. Ohmic resistance was measured at various stages in discharge by interrupting the current; *ir* polarization was recorded as a blanked-out portion on an oscilloscopic trace recording potential between test and reference. The shape of the discharge curve was found to be quite complex, consisting of a number of distinct regions, one of which was a plateau of fairly constant potential over an extended period of discharge time. This was quantitatively investigated in terms of Tafel type kinetics. An estimate of polarization observed in this region was corrected for *ir* and plotted versus log current density. Effects of temperature, electrode thickness, and current density on polarization in the plateau region were studied.

To investigate the distribution of reaction through porous electrodes, test electrodes were made by tightly stacking several of the above thin electrodes into the holder with a light dusting of silver powder between them to ensure good electronic contact. The test electrode was partially discharged at a set current density, removed from the cell, split into its component slices, and discharge completed separately on each component. Since the average coulombic capacity of Ag_2O initially present in each slice is known (4.9 ± 5%), and the coulombs remaining after partial discharge could be calculated from the completion of the discharge, the coulombs discharged in each section during the stacked test could then be readily calculated.

RESULTS

Galvanostatic discharge of the Ag-Ag_2O electrodes at low temperature and high current density showed that polarization passes initially through a pronounced peak and then reaches a plateau. After about 80% of the discharge has been completed, polarization increases very rapidly until the electrode is completely discharged. Some of these results have already been discussed (6). Only the results that pertain to the plateau region will be discussed in this paper. Values of polarization, corrected for *ir*, were obtained from the plateau region and were plotted versus log current density for electrodes of different thicknesses. Figure 5 shows experimental and predicted results for single and double thickness electrodes at −52°F. (−47°C.). The solid lines refer to the values predicted from the working equations using i_oS values estimated from the low current portion of the curve (normal Tafel region) and the circles are the actual experimental points. Similar results obtained at −35° and −80°F. and for electrodes of different thickness are also reported in Table 2. The electrodes are small discs cut from an inhomogeneous sheet, with a fresh electrode for each test; partly for this reason, the experimental data were not closely reproducible for duplicates. However, sufficient tests were performed to show the general pattern of results.

As discussed above, the prediction of the fraction of the total current supported by the reaction between 0 and x turns out to be dependent only on the ratio of the total applied current to i_c (Figure 3). Reaction in stacks of five electrodes is shown in Figure 6, where the fraction of reaction between 0 and x versus position in the electrode x/L is plotted for different i/i_c values. The solid lines represent the predicted values and the points are the actual data points. Table 3 gives the predicted versus experimental values of the percentage of reaction in each section of a stack of two electrodes as a function of i/i_c. The values of i_c were estimated as discussed in the next section.

DISCUSSION OF RESULTS

The discharge of the Ag_2O/Ag electrode proceeds via the overall reaction

$$Ag_2O(s) + H_2O + 2e^- \rightarrow 2Ag(s) + 2OH^-$$

where water is the reactant which must be transported from the bulk of the electrolyte through the pores of the electrode to the interior. Using the Austin ϕ criterion [Equation (8)], the value of ϕ for the test conditions described in this paper was estimated, assuming a value for the diffusion coefficient of water at room temperature of 2×10^{-5} sq.cm./sec., and assuming this diffusion coefficient to decrease with temperature in approximately the same ratio as the specific conductance of the electrolyte decreases. The values of specific conductance of the electrolyte as a function of temperature are known (7). This calculation gave a value of ϕ of approximately 4 at −52°F. and somewhat higher at room temperature. Because of the approximate nature of this calculation, and bearing in mind the experimental variability evident in the data, it was assumed that the results could be analyzed assuming ϕ to be sufficiently large that ohmic effects predominate over mass transfer effects. (If the particular value of $\phi = 4$ was included in the calculations of i_c and apparent exchange currents, results were not sufficiently different to alter the conclusions). Also, since water is present in high concentration, there is negligible effect of external mass transfer and $R_L/R_b = 1$.

For low values of η, but still large enough for irreversible reaction, the above theory of porous electrodes predicts that the total current density is approximated by $i = I_A \exp(\alpha\eta/b)$ where $I_A = i_oSL$. Thus a normal Tafel plot is obtained. The experimental results at low temperatures clearly indicate this Tafel line, with a transfer coefficient of approximately one-half. When reaction is concentrated toward the electrolyte face, a doubled Tafel slope is predicted, where the doubled slope intersects the normal Tafel line at i_c, where $i_c \sim 2b/\alpha\rho L$. Figure 5 shows a comparison of experimental and predicted results for a single (0.025 cm.) and double thickness electrode at −52°F. (−47°C.). Line a is drawn with a slope of 85 mv./current decade. The value of ρ can be estimated from $\rho = \rho_{free}\lambda$; for an electrode of 70% porosity, the labyrinth factor λ is about 2 and at −52°F., ρ_{free} is 40 ohm-cm. From the Tafel slope of 85 mv., $b/\alpha = 0.085/2.3 = 0.037$ v. Thus $i_c \sim (2)(0.037)/(0.0254)(40) = 73$ mamp./sq.cm.. Line b is drawn with a slope of 170 mv./current decade to cross line a at $i_c = 73$ mamp./sq.cm.. In addition, use of an electrode of twice the thickness should give results corresponding to line c, going into line b at a current of 73/2 = 36.5 mamp./sq.cm. The figure shows that the experimental points, both for the single and double thick electrodes, agree reasonably well with the predicted values. Since the experimental exchange current density of the normal Tafel region for a single thickness electrode is 0.3 mamp./sq.cm. (see Figure 5), i_oS is 12 mamp./sq.cm. Hence the apparent exchange current density of the doubled-Tafel slope region is $I_A \sim \sqrt{2i_oSb/\rho\alpha} = 4.7$ mamp./sq.cm., in good accordance with the value expected from Figure 5. It should be remembered that as the thickness of the electrode is increased, i_oSL increases, until the situation is reached where i_oSL approaches 4.7 mamp./sq.cm. Then a normal Tafel region would not be observed, and the near-reversible current versus polarization curve would change directly into the

Table 2. Predicted and Experimental Results of Polarization in Plateau Region as a Function of Temperature, Electrode Thickness, and Current Density

Electrode thickness, cm.	Temp., °F.	Current density, mamp./sq. cm.	i_c, mamp./sq. cm.	Polarization in plateau region, mv. Predicted	Experimental
0.05	−35	5	66.8	32	40
		10	66.8	60	45
		20	66.8	90	105
		30	66.8	105	115
		100	66.8	168	165
		150	66.8	200	195
0.025	−80	3	17.5	170	170
0.025		30	17.5	285	255/315*
0.025		80	17.5	340	320
0.125		150	3.5	385	360/390*

* Duplicates.

Table 3. Predicted Versus Experimental Values of Percentage of Reaction in Each Electrode Section

Temp., °F	Current density, mamp./sq. cm.	Electrode thickness, cm.	i/i_c	Percentage of reaction in electrode section: Back section Predicted	Back section Exptl.	Front section Predicted	Front section Exptl.
−35	150	0.050	2.25	29	24	71	76
−35	100	0.050	1.50	35	36	65	64
−35	30	0.050	0.45	42	40	58	60
−35	10	0.050	0.15	49	49	51	51
−52	50	0.050	1.35	35	43	65	57

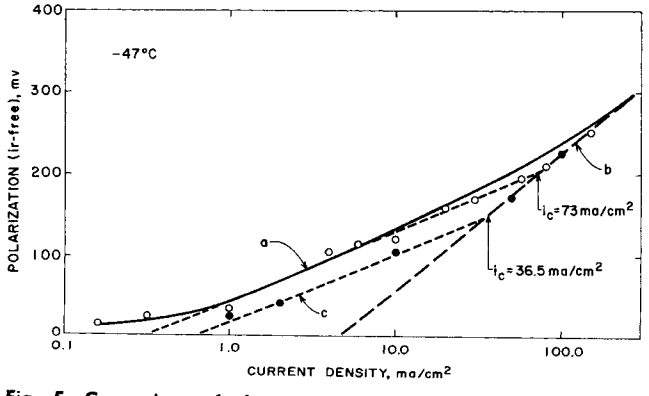

Fig. 5. Comparison of theoretical polarization with experimental points. ○, 0.025 cm. thick; ●, 0.050 cm. thick.

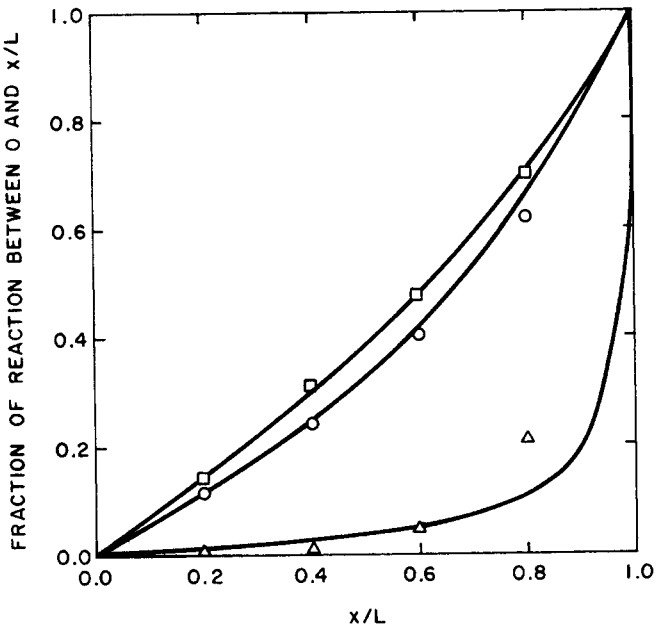

Fig. 6. A plot of predicted *(solid lines)* and experimental *(points)* values of $i(x)/i$ versus x/L for different i/i_c values. □ = i/i_c = 1.1; ○, i/i_c = 2.1; △, i/i_c = 42.

doubled-Tafel slope region as current density was increased.

Table 2 shows that the agreement between predicted and experimental results of polarization in the plateau region at other temperatures and for different electrode thickness is also quite good. To obtain the predicted values, the variation of exchange current density and specific resistance of the electrolyte with temperature must be known. At −52°F. the apparent exchange current density was $I_A = 0.3$ mamp./sq.cm. The exchange current density $(I_A)_T$ at any other temperature was calculated using

$$(I_A)_T = 0.3 \exp\left[\left(\frac{\Delta H^{+}}{R}\right)\left(\frac{T-226}{226T}\right)\right], \text{ mamp./sq.cm.}$$

where T is the absolute temperature (°K.); ΔH^{+} is the apparent activation energy for the reaction, which was found (*6, 8*) to be equal to 14.5 kcal./g.-mole; R is the gas constant. The specific resistance of the electrolyte varies from 1.5 to 80 ohm-cm. from 80° to −80°F. (*8*).

Figure 6 shows that the agreement between the predicted versus experimental values of $i(x)/i$ for stacks of five electrodes as a function of i/i_c is reasonably good. As expected, as the i/i_c ratio becomes smaller, the reaction becomes more uniformly distributed and approaches the limiting case where a plot of $i(x)/i$ versus x/L has a slope of 1. For an i/i_c value of about 42, the experimental results show that reaction is concentrated much more toward the electrolyte side of the electrode. Similar results obtained for double thickness electrodes are also shown in Table 2. Agreement between predicted and experimentally obtained results for electrodes of different thickness is good considering that the electrode does not actually operate at the steady state assumed in the theoretical equations. By the very nature of this type of electrode, the electrode changes during the reaction. In particular, of course, a high i/i_c value will force the exterior of the electrode to become completely discharged even when only a small fraction of the total coulombic capacity of the electrode has been used. Thus a discharged layer exists on the surface, which moves into the electrode as current continues to flow. This has the effect of reducing the active thickness of the electrode as far as distributed reaction is concerned.

CONCLUSIONS

The agreement between experimental and predicted results indicates that the concepts on which the theoretical treatments are based are sufficienly valid to be useful in practice. In particular, when external limiting current factors are not present, it is convenient to treat the current-polarization in three regions: near-reversible, normal Tafel slope, and doubled-Tafel slope. Such a treatment should normally be sufficiently accurate for design purposes. For example, for operation at low temperatures where the reaction is irreversible at useful currents, it is relatively easy to estimate the value of i_c for a given thickness and porosity of electrode. The thickness of the electrode should be chosen so that the maximum current density demand is less than i_c, since distributed reaction effects are not very pronounced for $i/i_c < 1$.

It is possible to insert the effect of external mass transfer if the mass transfer factors are known, by retaining the term $R(L)/R_b$ in the equations and replacing it as a function of i and the mass transfer factors.

Of course, the design of a complete cell or battery requires the optimization of a number of factors, which may be incompatible with the simple requirements given above for a single electrode. In addition, many electrode reactions of interest will be more complex than the straightforward case treated here. Work remains to be done especially on the transient equivalents to the steady state cases treated here.

NOTATION

b = RT/F in volts, R being gas constant, T absolute temperature
D = effective diffusion coefficient (including migration)
F = Faraday's constant
ΔH^{+} = apparent activation energy
i = current density at position x
i_c = crossover current [see Equation (16)]
i_o = exchange current density
I_A = apparent overall exchange current density
L = electrode thickness
n = electrons transferred per molecule of reactant
p = $\frac{\alpha}{b}\left(1+\frac{1}{\phi}\right)$
P = concentration of product dissolved in electrolyte
R = concentration of reactant dissolved in electrolyte
R_b, P_b = concentration of reactant and product, respectively, in undisturbed condition
S = specific reactive area, area per unit volume
V = conventional electrode potential
V_r = reversible electrode potential
x = position in the electrode

Greek Letters

α = electrokinetic transfer coefficient
η = polarization (departure from ideal reversible potential)
$\bar{\eta}$ = dimensionless polarization
ϕ = defined by Equation (8)
λ = labyrinth factor
ψ_E = potential of electrolyte
ψ_M = potential of electrode solid

ρ = effective specific resistance of electrolyte in electrode pores

LITERATURE CITED

1. de Levie, R., "Advances in Electrochemistry and Electrochemical Engineering," P. Delahay, ed., Vol. 6, Interscience, New York (1967).
2. Austin, L. G., Handbook of Fuel Cell Technology," C. Berger, Ed., p. 178, Prentice-Hall, Englewood Cliffs, N. J. (1968).
3. *Ibid.*, p. 138.
4. ———, *Trans. Faraday Soc.*, **60** (499), 1319 (1964).
5. ———, *Electrochim. Acta*, **14** (7), 639 (1969).
6. Gagnon, E. G. and L. G. Austin, *J. Electrochem. Soc.*, **118**, 479 (1971).
7. ———, "Handbook of Fuel Cell Technology," C. Berger, Ed., p. 141, Prentice-Hall, Englewood Cliffs, N. J. (1968).
8. Gagnon, E. G., Ph.D. thesis, Pennsylvania State Univ., University Park (1970).

Paper received March 18, 1970; paper accepted December 28, 1970.

Relative Velocities and Pressure Drops in Clouds of Drops, Bubbles, or Solid Particles

ISAAC YARON and BENJAMIN GAL-OR

Technion—Israel Institute of Technology
Haifa, Israel

Relative velocities of assemblages of drops or bubbles with respect to the continuous phase depend on many parameters. Generally, these include the densities and viscosities of both phases, the local acceleration, the size and shape of the particles, wall effects, concentration of particles and concentration of the practically ever-present surfactant impurities. The effect of the last two parameters on viscous flow in assemblages consisting of many spherical drops or bubbles (moving in an overall uniform velocity field) has been analyzed recently by Gal-Or and Waslo (*2*). Employing a free-surface cell model, they expressed their results in terms of the "ensemble" (ens.) relative velocity

$$U_{\text{ens.}} = \frac{3}{2} U_s \left(\Phi^{1/3} - \frac{Y}{W} \right) \tag{1}$$

where

$$W = 3 \left(1 + \frac{2}{3} \beta \right) + 2\Phi^{5/3} (1 - \beta) \tag{2}$$

$$Y = 2(1 + \beta) + 3\Phi^{5/3} \left(1 - \frac{2}{3} \beta \right) \tag{3}$$

$$\beta = \frac{\mu^c}{\mu^d + \gamma} = \frac{\mu^c}{\mu^d - \frac{1}{3} K(\partial\sigma/\partial\Gamma)} \tag{4}$$

and

$$K = \frac{2\Gamma_0 a}{2D_i^s + \alpha^* D_b^s a^2/[D_b^s + \alpha^* \delta(\partial\Gamma/\partial C)_{eq}]} \tag{5}$$

Here Φ is the volumetric fraction occupied by the particles and γ an interfacial viscosity due to surfactant impurities.

More recently, a zero-vorticity cell model has been employed by Gal-Or (*3*) to express ensemble relative velocity as

$$U_{\text{ens}} = -\frac{3}{2} U_s \left(W'\Phi - Y' + \frac{6}{5} \Phi^{1/3} \right) \tag{6}$$

where

$$W' = \frac{1}{3 + 2\beta} \left[\frac{2}{5} \Phi(1 - \beta) - 1 \right] \tag{7}$$

and

$$Y' = \frac{1}{3 + 2\beta} (\Phi + 2\beta + 2) \tag{8}$$

The aim of this paper is to evaluate an alternative definition of relative velocity and then to check which one may better characterize experimental data on viscous flow at low Reynolds numbers in dispersed systems. Employing the aforementioned models, we derive new formulations for the average relative velocity and pressure drop which may be widely applicable in characterizing viscous flows of drops or bubbles.

AVERAGE RELATIVE VELOCITY

The capability of Equations (1) and (6) to predict ensemble velocities is shown in Figure 1. Curves 1 to 4 are based on Equations (6), (1), (15), and (12), respectively; curves 6 and 7, on semitheoretical relations of Oliver (*12*) and Hawksley (*7*), respectively; curves 5 and 9 on experimental data of Adler and Happel (*1*) and Happel and Epstein (*5*), respectively; and curve 8 on experimental data of Hanratty and Bandukualka (*4*), Le Clair (*8*), and Lewis et al. (*10*). The theoretical predictions are, in general, lower than the experimental data.

Actual experimental data of this type are generally reported in terms of average relative velocity between the two phases involved (sometimes called the "slip" velocity). Comparison between experimental data and theoretical relations should, therefore, be carried out on this basis, rather than on the basis of $U_{\text{ens.}}$. The average relative velocity for a spherical cell model is defined by

$$\overline{U}_{\text{rel.}} = \frac{\int_{\phi=0}^{2\pi} \int_{\eta=0}^{\Phi^{-1/3}} [V_\theta^c]_{\theta=\pi/2} a^2 \eta d\eta d\phi}{\pi a^2 (\Phi^{-2/3} - 1)}$$

Correspondence concerning this article should be addressed to Prof. Benjamin Gal-Or who has also a joint appointment at the Chemical Engineering Department, University of Pittsburgh, Pittsburgh, Pa. 15213.